Hittite Journal of Science and Engineering, 2018, 5 (2) 137-140
ISSN NUMBER: 2148-4171
DOI: 10.17350/HJSE19030000085

Preparation of Silicon-Antimony Based Anode Materials for Lithium-Ion Batteries

Asuman Celik Kucuk Samet Ozturk Barış Cem Alpay, Mine Yorulmaz
Marmara University, Department of Metalurgical and Materials Engineering, Istanbul, Turkey

ABSTRACT

In this study, SixSb immiscible composite blend as anode materials have been synthesized using micron-sized silicone and antimony particles in different compositions through chemical reduction-mechanical alloying method (CR-MA). The obtained microstructures have been investigated by X-ray diffraction (XRD) and Scanning Electron Microscopy (SEM) with Energy Dispersive X-Ray analysis (EDX). Spectroscopic characterizations of the composite materials showed that a traditional intermetallic compound could not be achieved. However a novel immiscible composite blend system have been developed. One of the newly prepared composite materials, $Si^{0.65}Sb$, exhibits an initial capacity of 790 mAh g^{-1} and a good cyclic stability compared to the pure silicone. The battery performance results of the micron-sized $Si^{0.65}Sb$ blend system have been compared with the commercially used graphite and the nano-sized Si/Sb alloy systems. The cycling stability of the micron-sized $Si^{0.65}Sb$ blend system showed an improvement compared to nano-sized Si/Sb alloy systems. Moreover its specific capacity is slightly higher than the commercial graphite anode material. These results portray the importance of micron sized Si/Sb system in large-scale applications due to its low cost.

Article History:
Received: 2017/04/28
Accepted: 2017/12/04
Online: 2018/04/06

***Correspondence to**: Asuman Çelik Küçük*
Marmara University, Department of Metalurgical and Materials Engineering,
34722, İstanbul, Turkey
Tel: +90 (216) 348-02-92
Fax: +90 (216) 347-28-59
E-Mail: asuman.celik@marmara.edu.tr

Keywords: Silicon-Antimony based materials, Negative electrode, Li-ion battery

INTRODUCTION

The increased necessity for longer lasting and higher capacity batteries have led to the rapid development of lithium-ion batteries and their widespread use. This demand forces researchers to develop anode materials that could provide higher capacity along the numerous cycles [1]. Graphite, which is a commonly used anode material, has just 372 mAh g^{-1} initial theoretical capacity [2]. On the other hand, silicon is a promising anode material due to its high theoretical specific capacitance (4200 mAh g^{-1}). However Si faces drastic volume change up to 300% during lithiation and delithiation processes. Thus, silicon cannot retain its integrity during incessant battery cycles and this creates dead weight (inactive material) in battery [3]. To increase the cycling performance of Si-based anode materials, several approaches have been proposed in the literature such as; (1) developing nanostructured Si-based materials [4,5], (2) synthesis of Si-based alloy [6,7], and (3) preparation of amorphous silicon materials [8,9].

Among these, the approach of Si-based alloy system is comparable advantageous as it has a potential to prevent disintegration that occurs due to the volume expansion of silicon during the charge/discharge process. Therefore, several Si based alloy systems such as Si/C, Si/Ti, Si/Ni, Si/Fe [10-19] have been studied so far. Recently, Xinping Ai et al. developed a FeSi2/Si nanocomposite that exhibits a high Li storage capacity of ~1010 mAh g^{-1} and an excellent cyclability with 94% capacity retention after 200 cycles [18]. Martin Winter et al. synthesized porous NiSi2/Si/carbon composites [16], which resulted in good stability and high capacity.

Antimony (Sb) takes more attention due to great cycling stability even after numerous cycles [20]. However, the initial theoretical capacity of Sb is just 650 mAh g^{-1}. Therefore, in the Si/Sb alloy system, the high capacity of silicon can be combined with the high cyclic stability of antimony. According to our knowledge just one group, which is Jingwei Wang et al., have developed Si/Sb alloy system using nano-sized Si and Sb particles [21]. They claimed that SixSb immiscible alloy system have been succeeded by the chemical reduction-mechanical alloying method and found specific capacity of 1194 mAh g^{-1}. However after seven cycles, it drops to 596.4 mAh g^{-1}.

The motivation of this work is to obtain high capacity compared to the graphite anode material and cycling stability compared to the nano-sized Si/Sb alloy system. Therefore, alternative to nano-sized Si/Sb alloy system, micron-sized silicon and antimony particles have been utilized to develop Si/Sb alloy system by chemical reduction-mechanical alloying (CR-MA) method. However XRD, SEM-EDX studies displayed that alloying of Si and Sb in micron size cannot be succeeded but stable immiscible blend system can be. The battery performance results obtained from the micron-sized $Si^{0.65}Sb$ blend system have been compared to graphite and the nano-sized Si/Sb alloy system. It has been found that there is an improvement in cycling stability compared to nano-sized Si/Sb alloy system and in specific capacity compared to graphite anode material.

EXPERIMENTAL

Materials: Silicon powder (-100 mesh, 99.9% purity, density 2.329 g/cm^3), Antimony powder (-100 mesh, 99.5 % purity, density 6.697 g/cm^3), and absolute ethanol were purchased from Aldrich Chemical Co. Inc. and used as received. For battery tests; acetylene black, polyvinylidene fluoride (PVDF), and 1-methyl-2-pyrrolidinone (NMP) were kindly donated by Aldrich Chemical Co. Inc.

Preparation of Alloy: To obtain Si and Sb based alloy, chemical reduction and mechanical alloying method was used. Si and Sb mixed at different molar ratios into the attrition milling, while adding ethanol (300 ml) as milling control agents, charged with nitrogen as a protective gas. Samples were dried in a vacuum oven at 120 °C after milling process. Molar ratios, milling and drying times are shown in the Table 1.

Spectroscopic Characterization: XRD was performed using a Bruker AXS X-ray generator and diffractometer with Cu Kα radiation. The instrument operates at room temperature, with θ–2θ optics, and is equipped with a 3 kW generator and Cu Kα X-ray tubes. The system is interfaced with Visual XRD and Traces version 6.6.10 software designed for graphical processing and manipulation. The tube voltage and current were set at 40 kV and 25 mA, respectively.

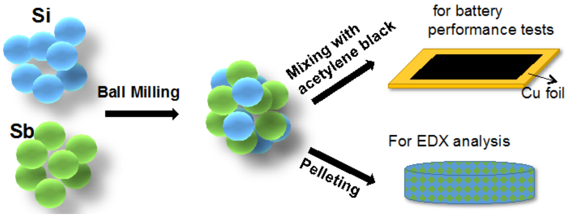

Figure 1. The concept and formation process of micron-sized Si/Sb blend system

Sample morphologies were investigated using a JEOL JEM-3000 (30 kV) SEM. Some of the higher resolution SEM images in this research work were obtained by using a field emission scanning electron microscope (FE-SEM), a JEOL JSM-7500FA. The elemental analysis of some particles was performed with energy dispersive X-ray spectroscopy (EDX).

Cell assembly and measurement: The electrode was prepared by mixing 70 wt% active materials, 10 wt% acetylene black and 20 wt% polyvinylidene fluoride (PVDF) binder in 1-methyl-2-pyrrolidinone (NMP) to form slurry, which was then spread onto a copper grid. Galvanostatic cycling measurements were performed with a classical two-electrode Swagelok-typeTM cell at a C/10 current density. Half-cell Li ion battery for test was assembled inside in an argon filled glove box to evaluate the electrochemical characteristics of $Si_{0.65}Sb$ alloy blend system. Ethylene carbonate (EC) and dimethyl carbonate (DMC) (EC/DEC: 1/1, V/V) was used as electrolyte and a porous polyethylene (PE) membrane was used as a separator. The cell was galvanostatically charged (Li+ insertion) and discharged (Li+ extraction) in the voltage range of 0.01–2.0 V vs Li/Li+ at different current densities at room temperature using VMP3 Biologic battery test system.

RESULTS AND DISCUSSION

Micron sized Si and Sb particles have been utilized to obtain Si/Sb alloy systems by CR-MA method. Si and Sb have been mixed at different molar ratios into the attrition milling, and obtained three different components. After milling process, samples have been dried in a vacuum oven at 120 °C. XRD, SEM-EDS and battery performance tests have been done for each SixSb blend system (Fig. 1).

XRD has been used to illuminate the microstructure of Si/Sb systems (Fig. 2). In the Fig. 2, the diffraction peaks of a series Si–Sb are attributed to Si and Sb phases. It has not

Table 1. Conditions of chemical reduction and mechanical alloying method and ratios of Si and Sb amounts in alloy samples

	Si	*Sb*	*Drying time (h)*	*Milling time (h)*
Experiment I/ $Si_{0.65}Sb$	*0.05 mol*	*0.08 mol*	*10*	*20*
Experiment II/ $Si_{0.85}b$	*0.06 mol*	*0.07 mol*	*10*	*20*
Experiment III/ SiSb	*0.07 mol*	*0.07 mol*	*10*	*20*

been observed any shift of Si and Sb peaks, meaning that traditional intermetallic compounds cannot be occurred. Jingwei Wang et al. have obtained same XRD result with that obtained in this study. However they investigated the peaks characteristic of Si-Sb immiscible alloy and observed an enhancement with the increasing Si contents, stating that an appropriate addition of Si contributes to the formation of Si-Sb immiscible alloy material [21]. However in this study, there is no relation between the peak areas of the elements in the X–ray diffraction spectroscopy and those of mixing ratios. Therefore, it has been concluded that alloying cannot be achieved using micron sized (100 mesh) silicone and antimony particles.

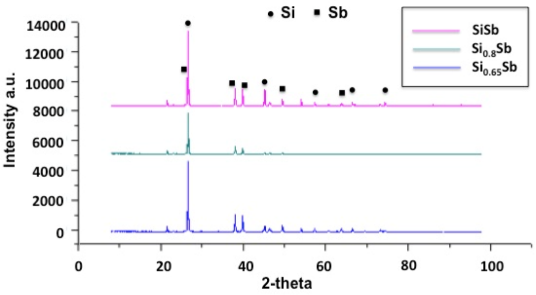

Figure 2. XRD patterns of Si-Sb immiscible blend system

Despite the preparation of three different samples, further experiments have been carried out for one specimen which is $Si_{0,65}Sb$ immiscible composite blend system.

The SEM image of $Si_{0.65}Sb$ immiscible blend system is showed in Fig.3. As schematically depicted in Fig. 3, the sample is formed by tiny irregular particles and the particles aggregated into homogenous secondary particles, which are uniformly distributed without distinct agglomeration.

An energy dispersive X-Ray analysis (EDX) is utilized to provide elemental identification and quantitative compositional information. Therefore further microstructure conformation has been done by SEM-EDX analysis (Fig. 4). The mixing ratio of Si:Sb in the $Si_{0.65}Sb$ immiscible blend system is 0.15 in weight. When the SEM-EDX analysis has been carried out for $Si_{0.65}Sb$, the normalised concentration ratio of the elements (Si:Sb) in weight percent is found to be 0.31. It has been clearly seen that no any relation between analysis results of the SEM-EDX and mixing ratios of Si and Sb powders. Aforementioned results obtained from XRD and EDX display that alloying of micron-sized Si and Sb particles cannot be achieved.

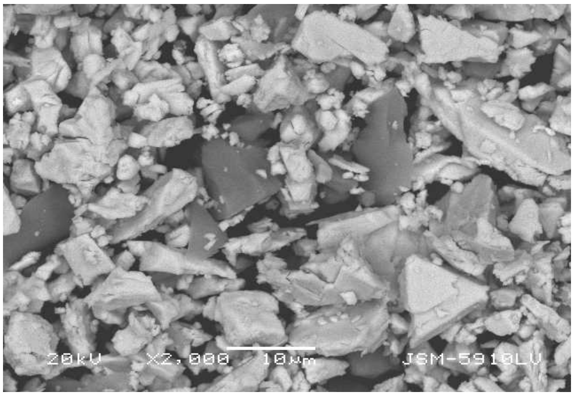

Figure 3. SEM image of $Si_{0.65}Sb$ immiscible blend materials.

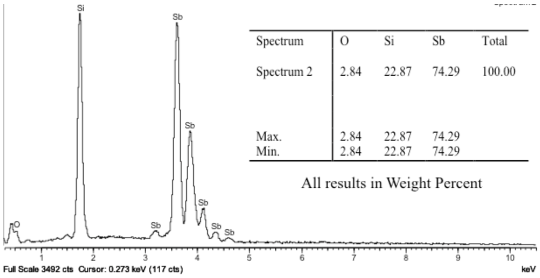

Spectrum	O	Si	Sb	Total
Spectrum 2	2.84	22.87	74.29	100.00
Max.	2.84	22.87	74.29	
Min.	2.84	22.87	74.29	

All results in Weight Percent

Figure 4. SEM-EDX result for Si0.65Sb blend system.

The prepared half–cell was galvanostatically charged (Li+ insertion) and discharged (Li+ extraction) in the voltage range of 0.01–2.0 V vs Li/Li+ to evaluate the electrochemical characteristics of $Si_{0.65}Sb$ alloy blend system at a C/10 (Fig. 5). Fig. 5 depicts the cycle performance of $Si_{0.65}Sb$ alloy anode material, providing a direct evidence of the good lithium storage performance due to the proper silicon contents.

The initial discharge capacity of the micron-sized $Si_{0.65}Sb$ anode material, which is obtained using the CR-MA method, is 790 mAh g^{-1} and the discharge capacity at the end of the 7th cycle is maintaining 520 mAh g^{-1} (Fig. 6). Although the initial specific capacity of the nano-sized Si/Sb alloy system is about 1194 mAh g^{-1}, its capacity drop to 596.4 mAh g^{-1} which means cycling stability of nano-sized Si/Sb alloy system is lower than micron-sized $Si_{0.65}Sb$ anode material. On the other hand, when the capacity values of the obtained $Si_{0.65}Sb$ anode material are compared with those of the conventional graphite anode material, it has been clearly seen that specific capacity of $Si_{0.65}Sb$ is higher than graphite anode material (Table 2)

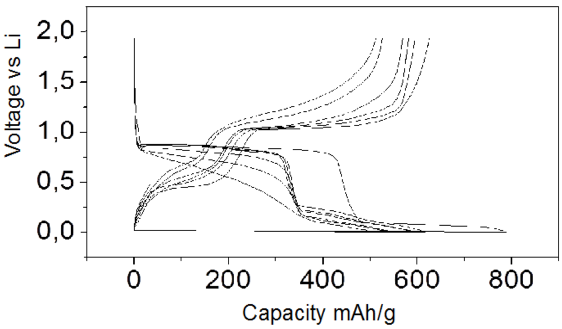

Figure 5. Initial charge–discharge curves of $Si_{0.65}Sb$ alloy anode material.

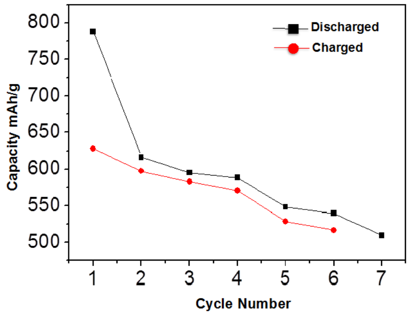

Figure 6. Cycle performance of $Si_{0.65}$Sb anode material in the potential range of 2.0 V – 0.01 V at a scan rate of 0.05 mV s^{-1} (vs. Li/Li+).

Table 2. Capacity comparision of $Si_{0,65}$Sb anode material with the literature.

Anode Materials	*1st cycling*	*7th cycling*
Graphite [25]	*372 mAh g^{-1}*	*350 mAh g^{-1}*
Silisium [26]	*4200 mAh g^{-1}*	*1580 mAh g^{-1}*
Antimony [27]	*650 mAh g^{-1}*	*200 mAh g^{-1}*
Nano-sized Sio,6Sb alloy [21]	*1194 mAh g^{-1}*	*596.4 mAh g^{-1}*
Micron-sized Sio,65Sb anode material [this study]	*790 mAh g^{-1}*	*520 mAh g^{-1}*

CONCLUSION

Stable immiscible blend systems composed of micron-sized silicon and antimony particles have been developed using CR-MA method. $Si^{0.65}$Sb blend system exhibits initial capacity of 790 mAh g^{-1} and a superior capacity of 520 mAh g^{-1} after 7 cycles. Although the blend system composes of micron size Si and Sb particles, which means interaction occurs in micron distances, the results are promising when compared to the nano-sized Si/Sb alloy system or to commercial using graphite.

ACKNOWLEDGEMENT

This work was financially supported by Marmara University scientific research projects FEN-A-150513-0173, FEN-E-120314-0064 and partially by the Scientific and Technological Research Council Of Turkey (TUBITAK). We thank Marmara University Scientific Research Project Unit (BABKO).

REFERENCES

1. Goodenough, J.B.; Park, K.S.; J. Am. Chem. Soc 2013, 135, 1167-1176
2. Horiba, T.; Maeshima, T.; Matsumura, Koseki, M.; Arai, J.; Muranaka, Y., Journal of Power Sources 2005, 146, 107–110.
3. Johnson, B. A.; White, R. E., Journal of Power Sources 1998, 70, 48–54.
4. Chan C.K., Peng H., Liu G., McIlwrath K., Zhang X.F., Huggins R.A., Nat Nanotechnol 2008, 3, 31 - 35.
5. Peng K.; Jie J.; Zhang W.; Appl Phys Lett 2008, 93, 033105.
6. Al–Maghrabi, M.A.; Thorne, J.S.; Sanderson, R.J.; Byers, J.N.; Dahn, J.R.; Dunlap, R.A.; J., Electrochem. Soc. 2012, 159, A119-A711.
7. Zhang, W.–J.; J. Power Sources 2011, 196, 13-24.
8. Yue, L.; Zhong, H.; Tang, D.; Zhang, L.; J. Solid State Electrochem. 2013, 17, 961- 968.
9. Astrova, E.V.; Fedulova, G.V.; Smirnova, I.A.; Remenyuk, A.D.; Kulova, T.L.; Skundin, A.M.; Technol. Phys. Lett. 2011, 37, 731-734.
10. Wang, M.S.; Fan L.Z.; J. Power Sources 2013, 244 570-574.
11. Zhang, K.; Zhao, Q.; Tao, Z.; J. Chen, Nano Res 2013, 6, 38-46.
12. Hu, Y.S.; Demir–Cakan, R.; Titirici, M.M.; Muller, J.O.; Schlogl, R.; Antonietti, M.; J. Maier, Angew. Chem. 2008, 47, 1645-1649.
13. Liu, W.R.; Yen, Y.C.; Wu, H.C.; Winter, M.; Wu, N.L.; J. Appl. Electrochem 2009, 39, 1643-1649.
14. Vadchenko, S.G.; Sytschev, A.E.; Kovalev, D.Y.; Shchukin, A.S.; Konovalikhin, S.V.; Nanotechnologies in Russia 2015, 10, 67-74.
15. Konovalikhin, S.V.; Kovalev, D.Y.; Sytschev, A.E.; Vadchenko, S.G.; Shchukin, A.S.; Int. J. Self–Propag. High–Temp. Synth 2014, 23, 217-221.
16. Jia, H.; Stock, C.; Kloepsch, R.; He, X.; Badillo, J.P.; Fromm, O.; Vortmann, B.; Winter, M.; Placke T.; ACS Appl. Mat. Interfaces 2015, 7, 1508-1515.
17. Wang, X.; Wen, Z.; Liu, Y.; Xu, X.; Lin, J.; Journal of Power Sources 2009, 189 121-126.
18. Chen, Y.; Qian, J.; Cao, Y.; Yang, H.; Ai, X.; ACS Appl. Mat. Interfaces 2012, 4, 3753-3758.
19. Park, H.; Lee, S.; Yoo, S.; Shin, M.; Kim, J.; Chun, M.; Choi, N.S.; Park, S.; ACS Appl. Mat. Interfaces 2014, 6, 16360-16367.
20. Huggins, R. A., Advanced Batteries: Materials Science Aspects 1sted.; Springer, LLC: New York, NY, 2009.
21. Wang, J.; Wang, Y.; Zhang, P.; Zhang, D.; Ren, X.; Journal of Alloys and Compounds 2014, 610, 308-314.
22. Deng, D.; Energy Science and Engineering 2015, 3, 385-418.
23. Horiba, T.; Maeshima, T.; Matsumura, Koseki, M.; Arai, J.; Muranaka, Y., Journal of Power Sources 2005, 146, 107–110.
24. Johnson, B. A.; White, R. E., Journal of Power Sources 1998, 70 48–54.
25. Kim, H.; Choi, J.; Sohn, H.J.; Kang, T.; J. Electrochem. Soc. 1999, 146(12), 4401-4405.
26. Moriga, T.; Watanabe, K.; Tsuji, D.; Massaki, S.; Nakabayashi, I.; J. Solid State Chem. 2000, 153(2), 386-390.
27. Roberts, G.A.; Cairns, E.J.; Reimer, J.A.; J. Power Sources 2002, 110(2), 424-429.